

Optical and electro-optic anisotropy of epitaxial $\text{Ba}_{0.7}\text{Sr}_{0.3}\text{TiO}_3$ thin films

D. Y. Wang,^{1,a)} S. Li,¹ H. L. W. Chan,² and C. L. Choy²

¹*School of Materials Science and Engineering, The University of New South Wales, Sydney, New South Wales 2052, Australia*

²*Department of Applied Physics and Materials Research Centre, The Hong Kong Polytechnic University, Hung Hom, Kowloon, Hong Kong*

(Received 7 September 2009; accepted 3 January 2010; published online 9 February 2010)

The anisotropic optical and electro-optic properties of ferroelectric $\text{Ba}_{0.7}\text{Sr}_{0.3}\text{TiO}_3$ thin films, deposited on highly transparent single-crystal MgO (001), (011), and (111) substrates using pulsed laser deposition, were investigated. The experimental results show a strong correlation between optical, electro-optic properties, and the orientation of $\text{Ba}_{0.7}\text{Sr}_{0.3}\text{TiO}_3$ thin films. The linear electro-optic coefficient r_c of the (001), (011), and (111)-oriented $\text{Ba}_{0.7}\text{Sr}_{0.3}\text{TiO}_3$ thin films are 99.1, 15.7, and 87.8 pm/V, respectively. Such a correlation may be attributed to the orientation dependent distribution and magnitude of spontaneous polarization. © 2010 American Institute of Physics. [doi:10.1063/1.3302453]

Complex ferroelectric oxide thin films with excellent optical properties and strong electro-optic (E-O) effects have now opened up the potential for guided-wave devices used in multifunctional integrated circuits.¹ Great efforts have been made to explore suitable ferroelectric oxide materials that have large E-O coefficient and can be epitaxially grown on low-refractive-index substrates.²⁻⁵ $\text{Ba}_{1-x}\text{Sr}_x\text{TiO}_3$ (BST), traditionally considered as a superior microwave dielectric material for application in wireless communication, has recently attracted much attention in the optoelectronic community because of its combination of high E-O coefficients,^{6,7} high optical clarity, and low optical loss.^{8,9} Furthermore, BST thin films have potential to overcome the major drawbacks of currently used E-O ferroelectric materials, such as the high cost and long optical path length of LiNbO_3 and LiTaO_3 single crystals and the environmental burden of lead content in $(\text{Pb},\text{La})(\text{Zr},\text{Ti})\text{O}_3$ transparent ceramics and thin films.

Anisotropy in ferroelectric materials has been intensively studied for years. The physical tensor, such as dielectric and piezoelectric properties in ferroelectric materials are closely correlated with the material's spontaneous polarization distribution. Optical properties of the ferroelectric thin films are expected to be anisotropic, since the spontaneous polarization has been switched due to the lattice distortion. We have previously reported the strain effect on E-O properties of $\text{Ba}_{0.7}\text{Sr}_{0.3}\text{TiO}_3$ thin films grown on various substrates.⁷ However, information pertaining to the optical and E-O anisotropy of BST thin films is limited. The understanding of orientation dependent optical properties of BST thin films is technically important for practical optoelectronic device development. In this letter, we investigated the optical (transparency, refractive index, and band gap energy) and electro-optic properties of $\text{Ba}_{0.7}\text{Sr}_{0.3}\text{TiO}_3$ thin films according to their crystalline orientations.

Orientation engineered $\text{Ba}_{0.7}\text{Sr}_{0.3}\text{TiO}_3$ thin films with surface normal orientations of (001), (011), and (111) have been epitaxially deposited on optically double-side polished single-crystal MgO (001), (011), and (111) substrates, re-

spectively, by pulsed laser deposition (PLD) using a KrF excimer laser (Lambda Physik COMPex 205) with a wavelength of 248 nm, a pulse width of 28 ns and a repetition rate of 10 Hz. The laser beam impacts the rotating stoichiometric target with an energy density of 2 J/cm². The distance between the target and the substrate was fixed at 5 cm, while the substrate temperature was maintained at 750 °C. All films were prepared by a fixed number of 6000 pulses in an oxygen atmosphere of 27 Pa. The growth conditions used in this work have been optimized and agreed well with reported data by other group.¹⁰

The crystal structures of the $\text{Ba}_{0.7}\text{Sr}_{0.3}\text{TiO}_3$ thin films were examined using an x-ray diffractometer (Bruker D8 Discover) equipped with Cu K α radiation. No secondary orientations and phases are detected from the $\theta/2\theta$ scans (figures not shown here), indicating the BST films are oriented along the particular normal of the substrates with a pure perovskite phase. The full width at half maximum of the x-ray rocking curves (ω scan) for the BST (001), (011), and (111) peaks of the (001), (011), and (111)-oriented BST films are 0.46°, 0.57°, and 1.06°, respectively, implying that the crystallites of all three films are fairly well ordered. The in-plane texturing of the BST thin films with respect to the major axes of the MgO substrates was confirmed by the XRD φ scan of the BST (110), (010), and (100) reflections of the (001), (011), and (111)-oriented BST films. The peaks from BST films coincide in position well with those from MgO substrates, as shown in Fig. 1, which suggests a nonlattice-rotated epitaxial growth of all the as-deposited BST films. For optical applications, epitaxial growth is desirable, since it can reduce light scattering due to a refractive index mismatch at grain boundaries.² Epitaxial growth is also necessary if the ferroelectric thin film is to have E-O properties comparable to the bulks.¹¹

Optical constants can be evaluated using the “envelop method” developed by Manificier *et al.*¹² For an insulating film on a transparent substrate, assuming the film is weakly absorbing and the substrate is completely transparent, the optical band gap energy E_{gap} , and refractive index n can be derived from the transmission spectra. The optical transmission of the $\text{Ba}_{0.7}\text{Sr}_{0.3}\text{TiO}_3$ thin films was measured using a Perkin Elmer (precisely) Lambda 950 UV-VIS spectrometer

^{a)} Author to whom correspondence should be addressed. Electronic mail: dy.wang@unsw.edu.au (D. Y. Wang). Tel.: +61 02 9385 4440. FAX: +61 02 9385 5956.

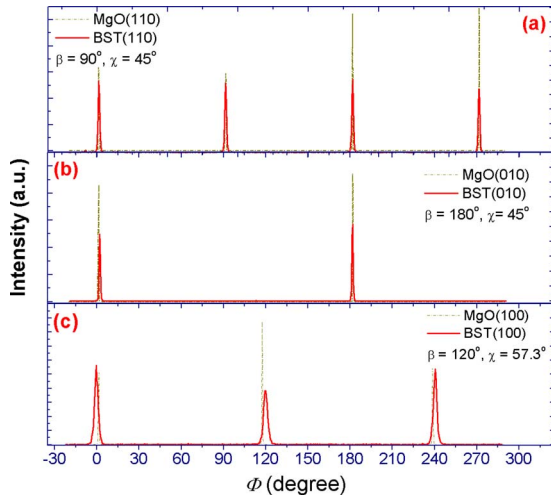


FIG. 1. (Color online) XRD ϕ scans of (a) $\text{Ba}_{0.7}\text{Sr}_{0.3}\text{TiO}_3$ (110) and MgO (110) reflections of (001)-oriented film (b) $\text{Ba}_{0.7}\text{Sr}_{0.3}\text{TiO}_3$ (010) and MgO (010) reflections of (011)-oriented film and (c) $\text{Ba}_{0.7}\text{Sr}_{0.3}\text{TiO}_3$ (100) and MgO (100) reflections of (111)-oriented film, providing nonlattice-rotating epitaxial growth of $\text{Ba}_{0.7}\text{Sr}_{0.3}\text{TiO}_3$ thin films.

in the wavelength range of 200–2000 nm. All three BST films are highly transparent in the visible to near infrared regions, as shown in Fig. 2, which is favorable for applications in optical communication (e.g., $\lambda=1.3$ and $1.5 \mu\text{m}$). The transparency of the films drops sharply in the UV region and the threshold wavelength is located at 311, 319, and 317 nm for (001), (011), and (111)-oriented films, respectively. The optical band gap energy E_{gap} of a thin film can be deduced from the spectral dependence of the absorption constant $\alpha(\nu)$ by applying the Tauc relation¹³

$$\alpha h\nu = \text{const}(h\nu - E_{\text{gap}})^{1/r}, \quad (1)$$

where ν is the frequency and h is the Planck's constant, $r=2$ for a direct allowed transition. The absorption constant $\alpha(\nu)$ is determined from the transmittance spectrum using the relation¹⁴

$$\alpha(\nu) = \left[\ln \frac{1}{T(\nu)} \right] / d, \quad (2)$$

where $T(\nu)$ is the transmittance at frequency ν and d is the film thickness. Thickness of the BST thin films were mea-

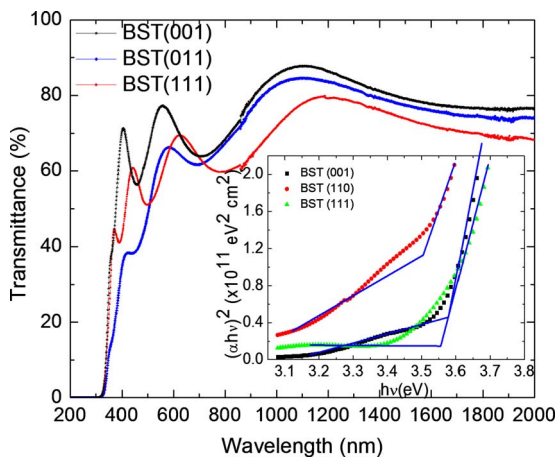


FIG. 2. (Color online) Optical transmission spectra of (001), (011) and (111)-oriented $\text{Ba}_{0.7}\text{Sr}_{0.3}\text{TiO}_3$ thin films. Inset is the plots of $(\alpha h\nu)^2$ vs $h\nu$ for $\text{Ba}_{0.7}\text{Sr}_{0.3}\text{TiO}_3$ thin films. The optical band gap energy E_{gap} is obtained by applying a “baseline” method.

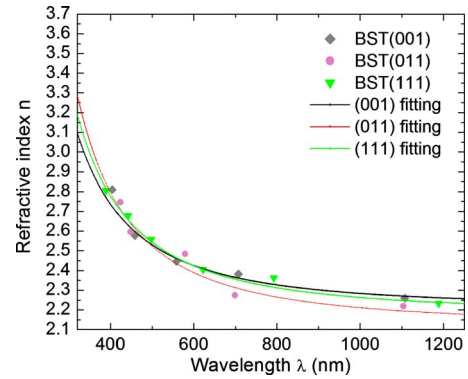


FIG. 3. (Color online) Variation of refractive indices of (001), (011), and (111)-oriented $\text{Ba}_{0.7}\text{Sr}_{0.3}\text{TiO}_3$ thin films as a function of wavelength. The solid lines are the fitting curves based on Cauchy equation.

sured by alpha-step profiler. [187, 193, and 225 nm for (001), (011), and (111)-oriented films, respectively]. The optical band gap energy is then obtained by applying a “base line” method¹⁵ in order to minimize the impact of reflectance losses at air-film and film-substrate interfaces. Inset of Fig. 2 shows the plots of $(\alpha h\nu)^2$ versus $h\nu$ for $\text{Ba}_{0.7}\text{Sr}_{0.3}\text{TiO}_3$ thin films grown on MgO substrates. The optical band gap energies are found to be 3.57 ± 0.01 , 3.50 ± 0.02 , and 3.55 ± 0.01 eV for (001), (011), and (111) oriented films, respectively. It is obviously that the absorption edges and optical band gap energy of the $\text{Ba}_{0.7}\text{Sr}_{0.3}\text{TiO}_3$ films are orientation dependent. Although the grain size effect on optical band gap energy of BST thin films has been reported,¹⁶ it is believed that orientation is the predominant factor that is responsible for the observed difference of E_{gap} in our case,¹⁷ as the average crystallites dimensions estimated by Scherrer's formula for the three films are comparable. Similar orientation dependence of band gap energy has also been observed in other oxygen-octahedral perovskite ferroelectrics, such as $\text{Pb}(\text{Mg}_{1/3}\text{Nb}_{2/3})\text{O}_3$ – PbTiO_3 , etc.¹⁷

The refractive index n of the as-deposited BST films was derived on the basis of the following expressions:¹²

$$n = \sqrt{N' + \sqrt{N'^2 - n_s^2}}, \quad (3)$$

$$N' = \frac{1 + n_s^2}{2} + \frac{2n_s(T_{\text{max}} - T_{\text{min}})}{T_{\text{max}}T_{\text{min}}} \quad (4)$$

in which T_{max} and T_{min} are the corresponding maximum and minimum of the envelop around the interference fringes at a certain wavelength λ , n_s is the refractive index of MgO, which is taken from Ref. 18 based on Sellmeier dispersion equation. The experimental values of the refractive index are found to fit closely to a Cauchy function as a formula

$$n = A + (B/\lambda)^2 + (C/\lambda)^4 \quad (5)$$

where A , B , and C are determined from fits to the experimental spectra. The calculated n and the dispersion of the refractive index for the three BST thin films were given in Fig. 3. The dispersion curves rise rapidly toward shorter wavelengths, showing the typical shape of dispersion near an electronic interband transition. Conspicuous orientation dependence of refractive index is discernable, especially in near infrared region. The (001)-oriented film exhibits the highest refractive index in near IR. The optical properties of an oxygen-octahedral ABO_3 perovskite ferroelectric are domi-

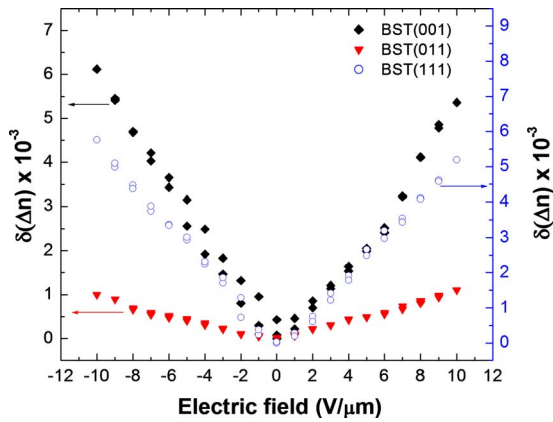


FIG. 4. (Color online) Change in birefringence $\delta(\Delta n)$ as a function of applied dc electric field for (001), (011), and (111)-oriented $\text{Ba}_{0.7}\text{Sr}_{0.3}\text{TiO}_3$ thin films. The birefringence was determined at a wavelength of 632.8 nm.

nated by BO_6 octahedra, which govern the low-lying conduction bands and the highest valence bands. This lowest energy oscillator is the largest contributor to the dispersion of the refractive index.¹⁹ Meanwhile, voids caused by surface roughness and porosity inside the film is another controlling factor for the variation of refractive index.^{19,20} Moreover, changes in electronic structure due to lattice distortion and some variations in atomic coordinate⁸ may also be responsible for the observed variation in refractive index of differently oriented BST thin films.

Electro-optic properties of the $\text{Ba}_{0.7}\text{Sr}_{0.3}\text{TiO}_3$ thin films were measured with a transverse geometry at the wavelength of 632.8 nm using modified Sénarmont method. Details of this method were presented in our previous work.⁷ The electrode pattern used for E-O characterization consisted of two gold coplanar electrodes, with dimensions $1.0 \times 8.0 \text{ mm}^2$ separated by a $20 \mu\text{m}$ wide gap. The film surface was set with the direction perpendicular to the incident light passing through the $20 \mu\text{m}$ electrode spacing and the electric field was applied normal to the incident light beam. The field induced birefringence of the thin films was measured as a function of dc electric field E at room temperature and the result is shown in Fig. 4, in which strong orientation dependence of E-O effect is clearly seen. E-O effect for the (011)-oriented film is relatively weak, while large birefringence changes $\delta\Delta n$ are revealed in (001) and (111)-oriented films. All the three films exhibit predominantly linear birefringence change with respect to the applied dc electric field. A slight hysteresis behavior is observed in the $\delta\Delta n$ versus E plots for (001)-oriented film, which is consistent with its enhanced ferroelectric properties.²¹ Generally, the birefringence shift due to linear E-O effect (Pockels effect) is given by Eq. (6) as following:

$$\delta\Delta n = \frac{1}{2} n^3 r_c E. \quad (6)$$

With this Eq. (6), the effective linear electro-optic coefficient r_c can be deduced from the slope of the $\delta\Delta n$ versus E plots. In this case, the linear E-O coefficient r_c of the (001), (011), and (111) oriented BST thin films were calculated to be 99.1, 15.7, and 87.8 p.m/V, respectively. The difference in E-O properties in the three kinds of oriented BST films may be attributed to the changes in distribution and magnitude of spontaneous polarization (electric) in orientation engineered films. The polarization changes could originate from: (1) the magnitude variation of the relative displacement of the Ti^{4+}

with respect to O^{2-} , (2) the change of domain growth mechanism, and (3) the lattice distortion caused by the stain in perovskite structure.^{5,10} Other factors, such as dielectric permittivity, may also be responsible for the orientation dependence of E-O effect in our tetragonal-distorted BST thin films.²² Further investigation needs to be conducted in order to clarify the underlying physics of the E-O anisotropy in BST films. Nevertheless, the linear E-O coefficients r_c of (001) and (111) oriented BST films are considerable higher than that of commonly used LiNbO_3 single crystals (30.8 pm/V),²³ showing their potential for use in active waveguide applications.

In summary, we reported a strong correlation between the optical, electro-optic properties and the crystalline orientation of epitaxial $\text{Ba}_{0.7}\text{Sr}_{0.3}\text{TiO}_3$ thin films grown on single-crystal MgO substrates by PLD. Understanding of the optical and electro-optic anisotropy in ferroelectric thin films is a critical issue for device design and fabrication. The refractive index and band gap energy were extracted from the transmission spectra of the thin films by employing an envelop method. The linear electro-optic coefficient r_c of the (001), (011), and (111)-oriented $\text{Ba}_{0.7}\text{Sr}_{0.3}\text{TiO}_3$ thin films were found to be 99.1, 15.7, and 87.8 pm/V, respectively. Our results suggested the (001) and (111)-oriented $\text{Ba}_{0.7}\text{Sr}_{0.3}\text{TiO}_3$ thin films are promising for integrated optics applications.

This work was partially supported by the Vice-Chancellor's postdoctoral fellowship program of the University of New South Wales (SIR50/PS16940). Financial support from the Centre for Smart Materials of the Hong Kong Polytechnic University is also acknowledged (1-A060/1-BB84).

¹B. W. Wessels, *Annu. Rev. Mater. Res.* **37**, 659 (2007).

²S. H. Lee, T. W. Noh, and J. H. Lee, *Appl. Phys. Lett.* **68**, 472 (1996).

³P. Tayebati, D. Trivedi, and M. Tabat, *Appl. Phys. Lett.* **69**, 1023 (1996).

⁴D. H. Kim and H. S. Kwok, *Appl. Phys. Lett.* **67**, 1803 (1995).

⁵Y. L. Lu, J. J. Zheng, M. C. Golomb, F. L. Wang, H. Jiang, and J. Zhao, *Appl. Phys. Lett.* **74**, 3764 (1999).

⁶J. W. Li, F. Diewer, C. Gao, H. Chang, X. D. Xiang, and Y. L. Lu, *Appl. Phys. Lett.* **76**, 769 (2000).

⁷D. Y. Wang, J. Wang, H. L. W. Chan, and C. L. Choy, *J. Appl. Phys.* **101**, 043515 (2007).

⁸H. Y. Tian, J. Choi, K. No, W. G. Luo, and A. L. Ding, *Mater. Chem. Phys.* **78**, 138 (2003).

⁹D. Y. Wang, H. L. W. Chan, and C. L. Choy, *Appl. Opt.* **45**, 1972 (2006).

¹⁰S. E. Moon, E. K. Kim, M. H. Kwak, H. C. Ryu, Y. T. Kim, K. Y. Kang, S. J. Lee, and W. J. Kim, *Appl. Phys. Lett.* **83**, 2166 (2003).

¹¹B. W. Wessels, *J. Electroceram.* **13**, 135 (2004).

¹²J. C. Manificier, J. Gasiot, and J. P. Fillard, *J. Phys. E* **9**, 1002 (1976).

¹³J. C. Tauc, *Optical Properties of Solids* (North-Holland, Amsterdam, 1972).

¹⁴E. A. Davis and N. F. Mott, *Philos. Mag.* **22**, 903 (1970).

¹⁵D. T. F. Marple, *Phys. Rev.* **150**, 728 (1966).

¹⁶R. Thielsch, K. Kaemmer, B. Holzapfel, and L. Schultz, *Thin Solid Films* **301**, 203 (1997).

¹⁷X. M. Wan, X. Y. Zhao, H. L. W. Chan, C. L. Choy, and H. S. Luo, *Mater. Chem. Phys.* **92**, 123 (2005).

¹⁸*Handbook of Optics*, 2nd ed. (McGraw-Hill, New York, 1994) Vol. 2.

¹⁹K. Y. Chan, W. S. Tsang, C. L. Mak, and K. H. Wong, *Phys. Rev. B* **69**, 144111 (2004).

²⁰S. H. Yang, D. Mo, H. Y. Tian, W. G. Luo, X. H. Pu, and A. L. Ding, *Phys. Status Solidi A* **191**, 605 (2002).

²¹D. Y. Wang, Y. Wang, X. Y. Zhou, H. L. W. Chan, and C. L. Choy, *Appl. Phys. Lett.* **86**, 212904 (2005).

²²X. M. Wan, H. S. Luo, X. Y. Zhao, D. Y. Wang, H. L. W. Chan, and C. L. Choy, *Appl. Phys. Lett.* **85**, 5233 (2004).

²³Y. Xu, *Ferroelectric Materials and Their Applications* (North-Holland, Amsterdam, 1991).